Nitrogen Activity Determination in Plasmas

A. BANDOPADHYAY, A. BANERJEE, and T. DEBROY

In many important materials processing operations, such as welding and plasma processing, a solid or a liquid metal is exposed to a plasma. In such systems, the activity of a species, such as nitrogen, in the plasma cannot be estimated from a straightforward application of the established thermochemical principles of gas-metal reactions. Currently, there is no established method for the determination of activity of a species in a plasma. In this article, a method for determination of nitrogen activity in plasmas is presented. High-purity tantalum and niobium samples were isothermally exposed to a well-characterized helium-nitrogen plasma, and the corresponding nitrogen solubility in each metal was determined by the vacuum fusion method. In each case, the activity of nitrogen in the plasma with respect to a standard state of 1 atm nitrogen pressure was calculated from the nitrogen solubility data and its value was demonstrated to be about an order of magnitude higher than the partial pressure of nitrogen in the source gas used to generate the plasma. The solubility of a species in a condensed phase exposed to a plasma can be used to determine its activity in the plasma.

I. INTRODUCTION

IN traditional thermochemical processing of metals and alloys, the feasibility of reactions, the activities of various species, and the solubility of gases in metals and alloys can be determined, in most cases, from the established principles and the available data base in metallurgical thermodynamics. However, such estimations are not possible for many important established and emerging materials processing operations where a solid or a liquid metal is exposed to a plasma. Some familiar examples include various types of welding and the laser, electron beam, and plasma processing of metals and alloys. Although plasmas are electrically neutral, the presence of excited neutral atoms, ions, and electrons precludes any simple extension of the well-established formal treatment of gas-metal systems to plasma-condensed matter systems.

Results of recent research at Penn State and elsewhere indicate that the physicochemical behavior of plasma-metal systems[1–5] is significantly different from that in the corresponding gas-metal systems. For example, when a pure metal, such as copper or iron, is exposed to a glow discharge argon plasma, its interfacial tension is significantly reduced.[3] The rates of vaporization of pure metal drops in a plasma environment are significantly lower[4,5] than those in the corresponding gas environment. Furthermore, the transformation of ordinary molecular species to excited neutral atoms and ions in the plasma leads to enhanced solution of species in metals. Uda *et al.*[6] and Ohno and Uda[7] have demonstrated that the concentrations of nitrogen in liquid iron and nickel during arc melting are significantly higher than the corresponding equilibrium solubilities when the metals are exposed to diatomic nitrogen molecules under non-arc melting conditions. Katz and King[8] also observed that, in the presence of an arc discharge, the concentration of nitrogen in liquid iron was significantly higher than the value predicted by Sievert's Law.

All of the previous works[6,7,8] on the solubility of a species in metals exposed to a plasma were conducted using electric arcs and relatively large quantities of metals. In these investigations, the metal in contact with the plasma jet was exposed to a strong radial temperature gradient, with the maximum temperature established at the jet axis. It is known from recent theoretical[9,10] and experimental[11] research that when a liquid metal is heated by an electric arc, the propagation of strong convection currents in the liquid pool due to Marangoni, densimetric, and electromagnetic effects is insufficient to eliminate the commonly present strong temperature gradient within the liquid. Inside the plasma jet, the highest absorption rate corresponds to the maximum surface temperature at the jet axis. Away from this axis, these rates change in a manner commensurate with the diminishing temperature profile. Outside the jet impingement area on a metal sample, a species can be either absorbed or desorbed in the metal depending on the local temperature and species concentration. Thus, a significant spatial variation of the local absorption rate is inevitable during absorption of a species in a metal from an environment containing an electric arc. Although a steady-state concentration of a species can be determined in such systems, the inevitable existence of a large temperature gradient precludes straightforward interpretation of the experimental data. Furthermore, in the previous investigations, no characterization of the plasma was undertaken, thereby making reproducibility and independent validation of such experiments difficult, if not impossible. However, in view of the enhanced species solubilities from plasmas, the need for systematic studies on the activity of various species in plasmas has become evident. The difficulties encountered in the interpretation of the results of the previous works can be overcome by conducting experiments with metal drops held isothermally in well-characterized plasmas.

Currently, there is no established method for the determination of the activity of a species in a plasma. In the work reported here, a method is proposed for the

A. BANDOPADHYAY, Postdoctoral Research Associate, A. BANERJEE, Graduate Student, and T. DEBROY, Professor, are with the Department of Materials Science and Engineering, The Pennsylvania State University, University Park, PA 16802.

Manuscript submitted July 29, 1991.

determination of nitrogen activity in plasmas. To demonstrate the procedure, niobium and tantalum samples were separately exposed to a well-characterized helium-nitrogen glow discharge plasma at a constant temperature, and the amounts of nitrogen in these metals were determined. The equilibrium concentration of nitrogen in either metal provides an indication of the nitrogen activity in the plasma with respect to the ground state molecular nitrogen at 1 atm pressure as the standard state. In principle, experiments may be conducted with only one of the two metals for the determination of nitrogen activity. However, since the metals do not significantly affect the properties of the plasma under the conditions of the experiments and the nitrogen activity in the plasma is independent of the metal, experiments with two different metals allow examination of the internal consistency of the data.

II. EXPERIMENTAL PROCEDURE

Thin, circular, disc-shaped samples of 1-mm ± 0.02-mm thickness were cut from niobium and tantalum sheets. The samples were polished and cleaned ultrasonically with acetone to remove contaminants such as grease and oil. The sample weights were 0.62 ± 0.03 and 0.81 ± 0.01 gm for niobium and tantalum, respectively. The initial nitrogen contents of the niobium and tantalum samples were 24 and 10 ppm, respectively.

A schematic diagram of the experimental setup is shown in Figure 1. The nitrogen plasma was generated inductively using a radio frequency (rf) generator capable of providing up to 10 kW power at 450 kHz. The rf power was supplied through a copper coil wound on a quartz reaction tube. A sample was placed on a tantalum wire specimen holder, which was specially designed to minimize sample-container contact area. To start the experiment, the system was evacuated and filled with a mixture of nitrogen and helium. The gases were allowed to flow through the system for 600 seconds. The sample was then heated to a temperature of 2243 K. The duration of the experiments was counted after the adjustment of temperature, which took less than 2 minutes. During the experiment, the sample was surrounded by an intense glow of plasma shown in Figure 2. After the experiment, the sample was cooled quickly by switching off power to the coil. Nitrogen and helium used in the experiments were of ultrahigh purity (99.999 pct). The supply of the gases to the reactor was controlled using electronic precision mass-flow controllers.

A two-color pyrometer with an internal calibration standard of 2273 K was used for the temperature measurements. The uncertainty of measurements using the two-color pyrometer is ±9 K. However, in practice, the accuracy of temperature measurement was limited to 20 K, which was the least count of the analog temperature display unit.

The samples were analyzed for nitrogen content using a LECO* TN-14 vacuum fusion analyzer. The uncertainty of the nitrogen analysis equipment was ±2 ppm. When this is combined with a ±3 ppm deviation of the calibration sample, the maximum estimated error is ±5 ppm. Since both Nb and Ta have very high nitrogen solubility, the error in the measurement of nitrogen content was insignificant.

*LECO is a trademark of LECO Corporation, St. Louis, MI.

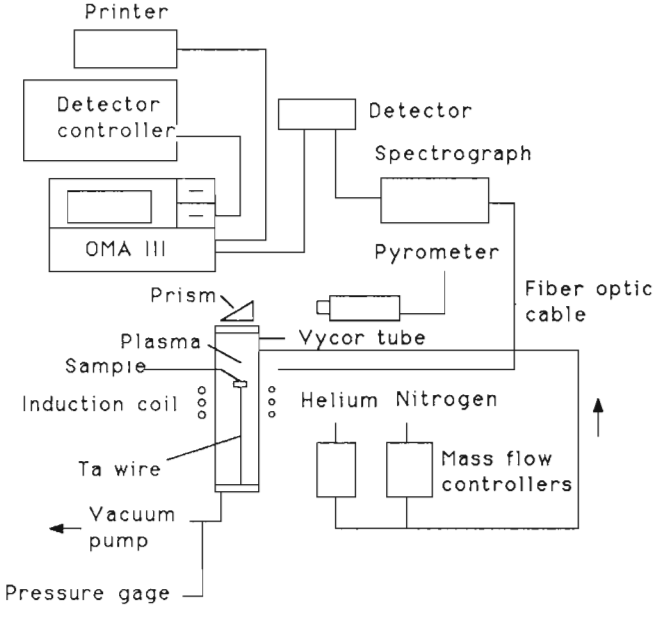

Fig. 1 — A schematic diagram of the experimental setup.

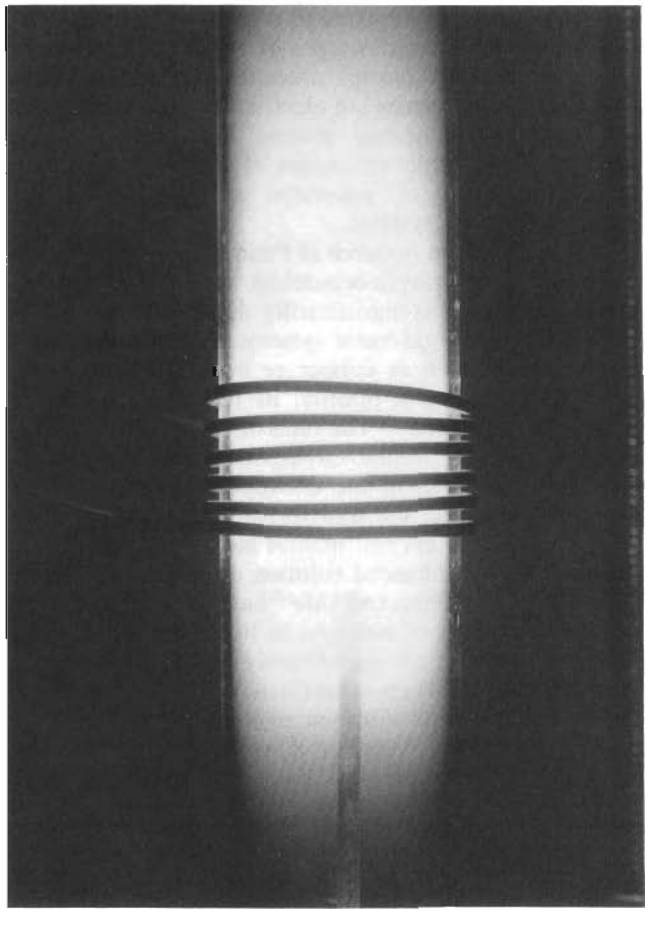

Fig. 2 — Glow discharge helium-nitrogen plasma.

Light emission from the plasma, shown in Figure 2, was analyzed using a Princeton Applied Research Corporation model 1253 digital triple-grating spectrograph and an OMA* III optical multichannel analyzer system. The light emissions were transmitted to the spectrograph using optical fibers. A 150 grooves/mm diffraction grating was used for scanning a large wavelength range for the identification of the various species in the plasma. However, for collecting data on intensity *vs* wavelength, a 1200 grooves/mm diffraction grating was employed to achieve high peak resolution. Wavelength calibration was achieved using argon, neon, and mercury calibration lamps.

*OMA is a trademark of EG&G Princeton Applied Research, Princeton, NJ.

III. RESULTS AND DISCUSSION

Since the partial pressure of nitrogen in the plasma source gas does not uniquely define the environment from which nitrogen is absorbed in the metal, characterization of plasma is crucial for defining the experimental conditions. The nature of the excited and ionized species and the average kinetic energy (temperature) and population density of the electrons in the plasma were determined prior to nitrogen solubility measurements.

A. *Excited and Ionized Species*

Figures 3 and 4 represent typical optical emission spectra for the nitrogen-helium plasma used in the experiments. A listing of the various species detected in the plasma, the transition states involved[13,14] in the light emission, and the corresponding wavelengths are presented in Table I. The symbols for denoting the transition states used in this table consist of the electronic

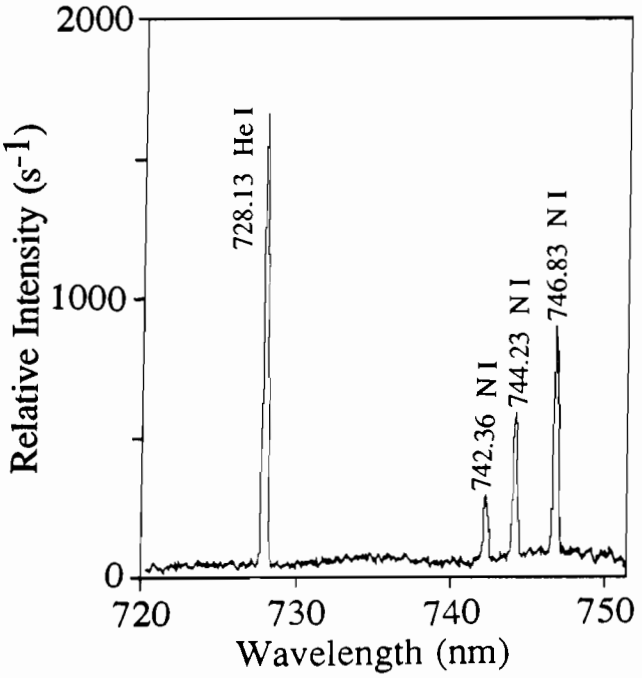

Fig. 3—Intensity *vs* wavelength in the 720 to 750 nm range.

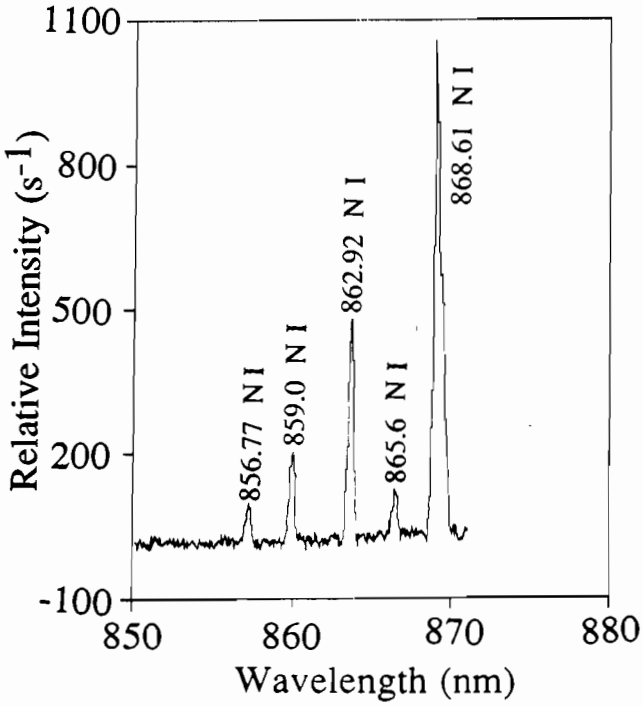

Fig. 4—Intensity *vs* wavelength in the 850 to 880 nm range.

configuration, such as $2p^2 3s$, and the term symbol expressed within the first bracket, such as (^4P). The letter in the term symbol, such as P, indicates total orbital angular momentum, and the superscript, such as 4 in ^4P, indicates multiplicity, *i.e.*, the number of energy levels depending on the spin of the electrons. Thus, the combination of the configuration and the term symbol precisely denotes the energy levels of the electrons. It is observed from the table that the plasma contains nitrogen atoms and molecules in both their excited and ionized states and excited helium and niobium atoms. No N^{3+} ions were detected from the spectra. Shahin[12] has shown by mass spectroscopic studies that the concentration of N^{3+} ions in a nitrogen plasma is less than 1 pct of the total ions present. Since the extent of ionization in the plasma is small, the detection of N^{3+} ions is difficult. A discussion about the various collision processes involved in the formation of the species detected in the plasma by emission spectroscopy is presented in Appendix I.

B. *Electron Temperature*

The average kinetic energy of the electrons, expressed as the electron temperature, was determined from the intensity *vs* wavelength data presented in Figures 3 and 4. The calculation procedure is available in standard textbooks such as Boumans.[16] Therefore, only a brief outline of this procedure is presented here. The combination of the equation for absolute intensity of an atom line with an expression for the Boltzmann distribution of energy level populations yields an expression of the following form:

$$\ln (I/gAv) = \ln C - (E_q/kT) \qquad [1]$$

where I is the integrated intensity in s^{-2}, g is the degeneracy of the upper energy level q, A is the transition

Table I. Light-Emitting Species Detected During Exposure of a Niobium Sample in the Nitrogen-Helium Glow Discharge Plasma

Species	Electronic Transition State[13,14]	Wavelength (nm)
N excited (N I)	$2p^23s\ (^4P)\text{-}2p^2\ (^3P)\ 3p\ (^4S^0)$	742.36
	$2p^23s\ (^4P)\text{-}2p^2\ (^3P)\ 3p\ (^4S^0)$	744.23
	$2p^23s\ (^4P)\text{-}2p^2\ (^3P)\ 3p\ (^4S^0)$	746.83
	$2p^23s\ (^4P)\text{-}2p^2\ (^3P)\ 3p\ (^4P^0)$	818.48
	$2p^23s\ (^4P)\text{-}2p^2\ (^3P)\ 3p\ (^4P^0)$	820.03
	$2p^23s\ (^4P)\text{-}2p^2\ (^3P)\ 3p\ (^4P^0)$	821.07
	$2p^23s\ (^4P)\text{-}2p^2\ (^3P)\ 3p\ (^4P^0)$	821.63
	$2p^23s\ (^4P)\text{-}2p^2\ (^3P)\ 3p\ (^4P^0)$	822.31
	$2p^23s\ (^4P)\text{-}2p^2\ (^3P)\ 3p\ (^4P^0)$	824.23
	$2p^23s\ (^2P)\text{-}2p^2\ (^3P)\ 3p\ (^2P^0)$	856.77
	$2p^23s\ (^2P)\text{-}2p^2\ (^3P)\ 3p\ (^2P^0)$	859.00
	$2p^23s\ (^2P)\text{-}2p^2\ (^3P)\ 3p\ (^2P^0)$	862.92
	$2p^23s\ (^2P)\text{-}2p^2\ (^3P)\ 3p\ (^2P^0)$	865.59
	$2p^23s\ (^4P)\text{-}2p^2\ (^3P)\ 3p\ (^4P^0)$	868.61
N ions (N II)	$2p3s\ (^1P^0)\text{-}2p\ (^2P^0)\ 3p\ (^1P)$	648.21
	$2p3d\ (^3D^0)\text{-}2p\ (^2P^0)\ 4p\ (^3D)$	653.25
	$2p3d\ (^3D^0)\text{-}2p\ (^2P^0)\ 4p\ (^3D)$	654.42
He excited (He I)	$1s2s\ (^3S)\text{-}1s3p\ (^3P^0)$	388.87
	$1s2s\ (^1S)\text{-}1s4p\ (^1P^0)$	396.47
	$1s2p\ (^3P^0)\text{-}1s5d\ (^3D)$	402.62
	$1s2p\ (^3P^0)\text{-}1s4d\ (^3D)$	447.15
	$1s2p\ (^3P^0)\text{-}1s4s\ (^3S)$	471.32
	$1s2p\ (^1P^0)\text{-}1s4d\ (^1D)$	492.20
	$1s2s\ (^1S)\text{-}1s3p\ (^1P^0)$	501.56
	$1s2p\ (^1P^0)\text{-}1s4s\ (^1S)$	504.77
	$1s2p\ (^3P^0)\text{-}1s3d\ (^3D)$	587.57
	$1s2p\ (^1P^0)\text{-}1s3d\ (^1D)$	667.82
	$1s2p\ (^1P^0)\text{-}1s3d\ (^1S)$	728.13
N_2 excited	$C^3\pi - B^3\pi$	326.85
	$C^3\pi - B^3\pi$	328.53
	$C^3\pi - B^3\pi$	330.90
	$C^3\pi - B^3\pi$	353.67
	$C^3\pi - B^3\pi$	364.17
	$C^3\pi - B^3\pi$	371.05
N_2^+ ioinized	$^2\Sigma - 2\Sigma$, ground state	329.34
	$^2\Sigma - 2\Sigma$, ground state	329.90
	$^2\Sigma - 2\Sigma$, ground state	356.39
	$^2\Sigma - 2\Sigma$, ground state	391.44
Nb excited (Nb I)	—	375.96
	—	381.10
	—	382.49
	—	392.50
	—	661.67

probability for the transition from the upper energy state q to the lower energy level in s^{-1}, v is the frequency in s^{-1}, E_q is the energy associated with the level q in cm^{-1}, k is the Boltzmann constant in $cm^{-1}\ K^{-1}$, T is the electron temperature in Kelvin, and C is a constant. The electron temperature can be obtained from the slope of the plot with the left-hand side of Eq. [1] *vs* E_q. The data used for the calculations[13] and a sample calculation are presented in Table II and Appendix II, respectively. Figure 5 shows the Boltzmann plot obtained from the spectral data of the excited helium atom peaks obtained during exposure of Nb in the plasma. For the plasma investigated in our experiment, the electron temperature was found to be 4455 K or 0.6 ev. This value is close to the lower end[16] of the electron temperature range for glow discharge plasmas.

C. *Electron Density and Degree of Ionization*

It is demonstrated in Appendix III that the Doppler broadening is not important under the conditions of the experiments reported in this article. The electron density in the plasma was evaluated from the Stark broadening of the peaks. The procedure does not require assumption of local thermodynamic equilibrium and is a reliable method for the determination of the electron density. The electron density,[17] in cm^{-3}, can be related to the full half width, $\Delta\lambda_s$, as

$$N_e = C(N_e, T)\Delta\lambda_s^{3/2} \qquad [2]$$

where $C(N_e, T)$ is a weak function of temperature and electron density. The data used for the calculations and the results are presented in Table III.

The electron density has also been calculated from a different relationship suggested by Wiese:[18]

$$\Delta\lambda_{1/2} = 2.5 \times 10^{-9}\alpha_{1/2}N_e^{2/3} \qquad [3]$$

where $\Delta\lambda_{1/2}$ is the full half width in Angstroms and $\alpha_{1/2}$ is the value of α in Angstroms per CGS field strength unit at which the reduced Stark profile, $S(\alpha)$, is at one half of its maximum value. The electron densities calculated from Eq. [3] are also given in Table III. It is observed that the calculated electron densities from these two relationships agree fairly well, and the average electron density is $2.54 \times 10^{15}\ cm^{-3}$. The corresponding degree of ionization, which is the ratio of the electron density to the density of the atoms and molecules, is 7×10^{-2}. This value is somewhat higher than the value commonly reported[19] for glow discharge systems which, unlike the system used in the present investigation, usually do not contain metal vapor.

D. *Nitrogen Activity in the Plasma*

The concentration *vs* time plots for the dissolution of nitrogen in tantalum and niobium at 2243 K from the plasma are presented in Figures 6 and 7, respectively. The nitrogen partial pressure in the source gas from which the plasma was generated was 1.12 Pa (1.11×10^{-5} atmosphere). The corresponding equilibrium nitrogen solubility levels under non-plasma condition are shown by the dotted lines in the figures. These equilibrium nitrogen solubility values were calculated from the relationship recommended by Fromm and Jehn[20] for Ta and from the results of Fromm and Jehn[20] and Elyutin *et al.*[21] for Nb. It is observed from Figures 6 and 7 that when either metal was exposed to the nitrogen-helium plasma, the nitrogen solubility was found to be about three times higher than what was expected in a diatomic gas environment from which the plasma was formed.

The dissolution of nitrogen in solid metal samples can be expressed as

$$1/2N_2\ (g) = \underline{N}(M,s) \qquad [4]$$

where "M" designates a metal and "s" represents a solid

Table II. Data Used for the Computation of Electron Temperature*

λ (nm)	$\Delta\nu$ (s^{-1})	CF	I_r (s^{-1})	I (s^{-2})	g	A (s^{-1}) ($\times 10^8$)	E_q (cm^{-1})	ln ($I/gA\nu$)
388.9	1.35×10^{12}	1.6	7232	7.6×10^{15}	9	0.095	185,565	−15.97
396.5	1.30×10^{12}	1.5	295	2.9×10^{14}	3	0.072	191,493	−17.85
402.6	1.25×10^{12}	1.5	535	5.0×10^{14}	15	0.117	193,917	−19.38
447.2	1.26×10^{12}	1.2	3224	2.4×10^{15}	15	0.251	191,445	−18.45
471.3	8.10×10^{11}	1.1	537	2.3×10^{14}	3	0.106	190,298	−18.27
492.2	8.42×10^{11}	0.99	1667	6.9×10^{14}	5	0.202	191,447	−18.30
501.6	8.10×10^{11}	0.95	5095	2.0×10^{15}	3	0.134	186,210	−16.32
504.8	5.94×10^{11}	0.93	143	3.9×10^{13}	1	0.066	190,940	−18.41
587.6	7.86×10^{11}	0.75	68,095	2.0×10^{16}	15	0.706	186,102	−17.11
667.8	4.57×10^{11}	0.88	30,294	6.0×10^{15}	5	0.638	186,102	−16.98
728.1	5.17×10^{11}	1.6	1619	5.3×10^{14}	1	0.181	184,865	−16.45

*The values of g, A, and E_q are taken from Ref. 13. The symbol λ is the wavelength, $\Delta\nu$ is the difference in frequency at the base of the peak, CF is the correction factor for the intensity, and I_r is the relative intensity. All other symbols are explained in the text. A sample calculation for determining ln ($I/gA\nu$) is presented in Appendix II.

phase. For the dissolution of nitrogen from a plasma, Eq. [4] should be regarded as a symbolic representation rather than an overall reaction, since in addition to molecular nitrogen of various energy states, atomic and ionic species are also present in the plasma. Indeed, it will be demonstrated subsequently in this article that the solubility of nitrogen in the metals in the plasma environment is significantly higher than that in a non-plasma molecular nitrogen source gas. For nitrogen dissolution from diatomic nitrogen, the activity of nitrogen in the gas phase is equal to $(p_{N_2})_g$, the partial pressure of nitrogen in the gas phase. However, the equivalent activity of nitrogen in the plasma, $(a_{N_2})_p$, is not equal to the partial pressure of nitrogen in the plasma source gas. The equilibrium constant, K, for Reaction [4] is given by the following expression:

$$K = (\text{wt pct } \underline{N})_p/(a_{N_2})_p^{1/2} = (\text{wt pct } \underline{N})_g/(p_{N_2})_g^{1/2} \quad [5]$$

where the subscripts p and g represent plasma and the plasma source gas, respectively. At 2243 K, the values[20] of K are 95.8 and 46.5 for tantalum and niobium, respectively. The activity of nitrogen in the plasma with respect to a hypothetical standard state of 1 atm pressure of diatomic nitrogen gas is given by

$$(a_{N_2})_p = [(\text{wt pct } \underline{N})_p/K]^2 \quad [6]$$

In the plasma formed from a gas with $p_{N_2} = 1.12$ Pa (1.11×10^{-5} atm), the nitrogen activity values, $(a_{N_2})_p$, calculated from the experimentally determined nitrogen solubility data in the plasma environment for Ta and Nb are 1.06×10^{-4} and 1.20×10^{-4}, respectively. The ratio of the activities of nitrogen in the plasma and the plasma source gas is given by the following:

$$R = (a_{N_2})_p/(p_{N_2})_g \quad [7]$$

The calculated values of R for Ta and Nb are 9.5 and 10.8, respectively. The data show the uniqueness of the nitrogen activity in the plasma irrespective of the metal samples used. Thus, the activity of nitrogen in the low-pressure glow discharge nitrogen-helium plasma used in the experiments is about ten times the partial pressure of nitrogen in the source gas from which the plasma was formed.

The solubility of nitrogen in niobium in the presence of a plasma is plotted as a function of the square root of the nitrogen partial pressure in the plasma source gas in Figure 8. The total pressure in all experiments was maintained constant at 147 Pa (1.45×10^{-3} atm). For all

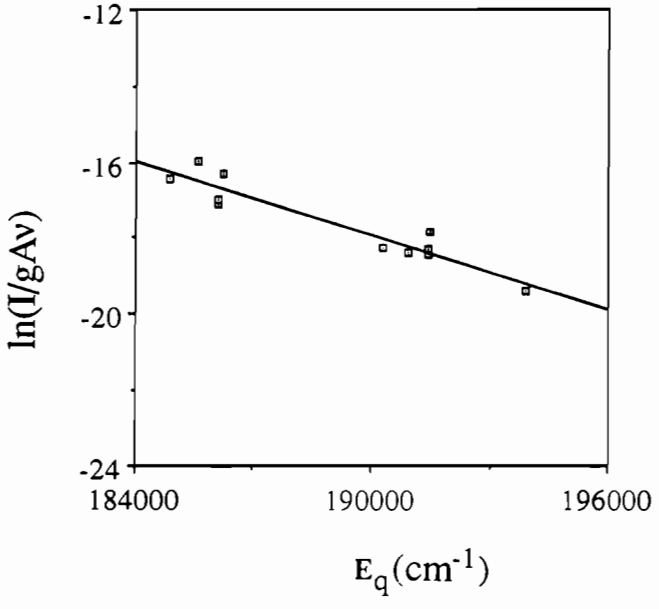

Fig. 5—Boltzmann plot for the glow discharge He-N plasma.

Table III. Electron Density in Helium-Nitrogen Plasma

Peak Wavelength (nm)	Full Stark Width (Å)	$C(N_e, T)$[16]	$\alpha_{1/2}$[16]	$N_e \times 10^{-15}$, cm^{-3} Eq. [2]	Eq. [3]
396.5	2.04	9.99×10^{14}	0.04	2.91	2.91
447.2	2.99	4.15×10^{14}	0.07	2.14	2.23

Total pressure, atm	1.45×10^{-3}
Partial pressure of N_2, atm	1.11×10^{-5}
Electron temperature, K	4455
Number density of atoms and molecules, cm^{-3}	3.57×10^{16}
Average electron density, cm^{-3}	2.54×10^{15}
Degree of ionization	7×10^{-2}

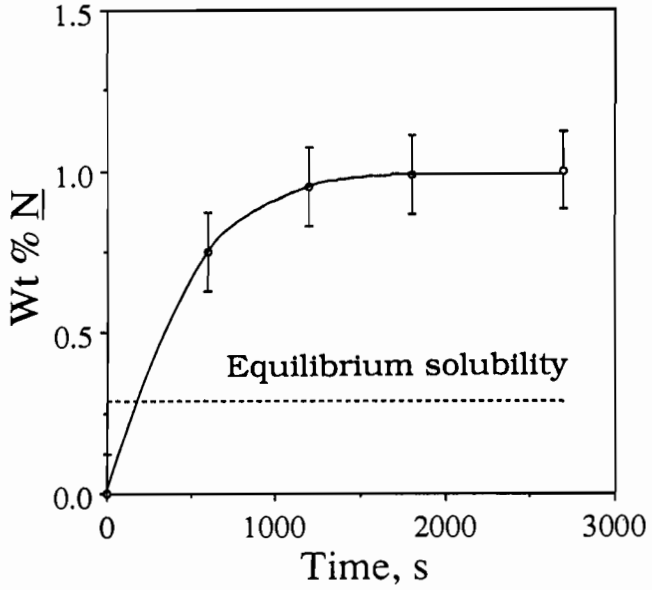

Fig. 6—Weight percent N *vs* time plot for dissolution of nitrogen at 2243 K in Ta.

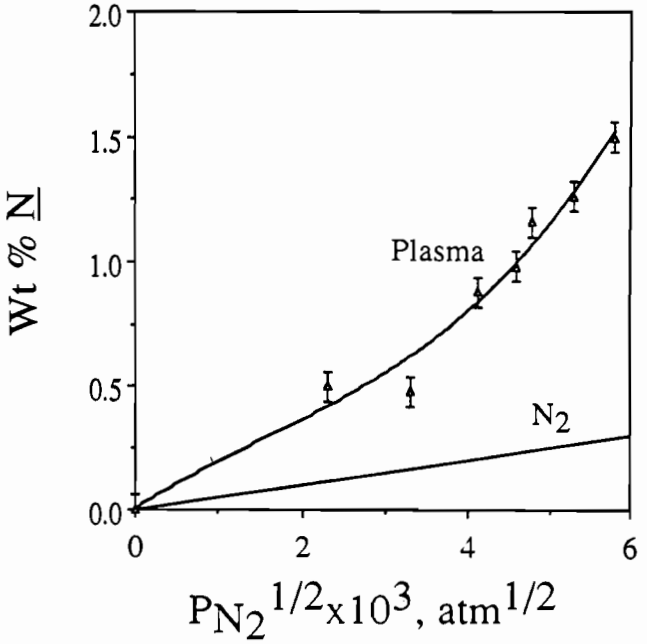

Fig. 8—Weight percent N *vs* $p_{N_2}^{1/2}$ plot for dissolution of nitrogen at 2243 K in Nb.

experiments, the solubility of nitrogen in niobium from the plasma environment is higher than that from the molecular nitrogen. Furthermore, the ratio of the nitrogen solubilities in niobium exposed to the plasma and the nonplasma systems increased with the partial pressure of nitrogen in the plasma source gas.

The enhanced solubility must be attributed to the presence of one or more of the species present in the plasma other than the diatomic nitrogen, *i.e.*, neutral nitrogen atoms, ions, and electrons. Since these species originate from inelastic collisions between energetic electrons and nitrogen molecules, the frequency of such collisions should be considered to be the primary contributor in achieving the enhanced solubility of nitrogen in the plasma environment. Therefore, for a discussion of the results presented in Figure 8, let us consider the rate of inelastic collisions, r, between energetic electrons and nitrogen molecules as follows:[22]

$$r = kn_e n_{N_2} \qquad [8]$$

where k is a rate constant, n_e is the electron density, and n_{N_2} is the concentration of the N_2 molecules. Since the ratio of the electric field strength to pressure did not vary with nitrogen partial pressure in these experiments, the electron temperature was constant in these experiments.[23] Therefore, under the conditions of the experiments, the rate constant k can be taken as a constant. However, the electron density, n_e, increases with the higher concentration of nitrogen. As a result, the rate of inelastic collisions between the energetic electrons and the nitrogen molecules increases at a rate higher than the rise in the concentration of the nitrogen molecules. Thus, the enhancement in the nitrogen solubility in Figure 8 with the nitrogen partial pressure is consistent with the importance of the collision between the electrons and the nitrogen molecules.

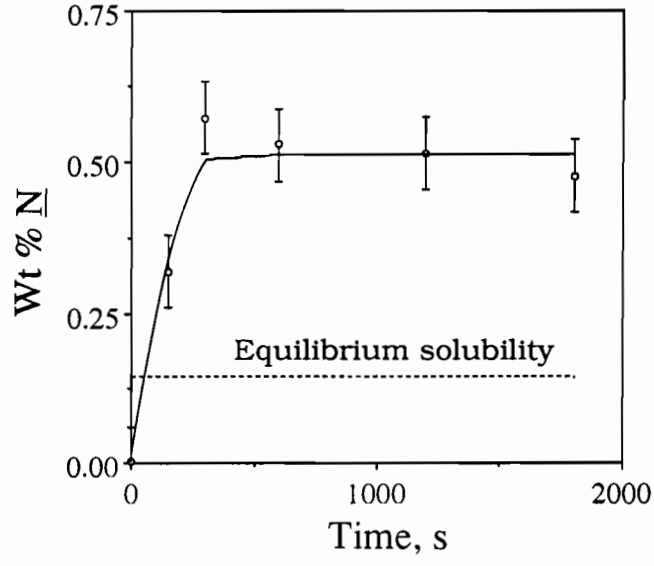

Fig. 7—Weight percent N *vs* time plot for dissolution of nitrogen at 2243 K in Nb.

IV. SUMMARY AND CONCLUSIONS

A method for the determination of nitrogen activity in a plasma is demonstrated. The activity of nitrogen in a glow discharge nitrogen-helium plasma was evaluated from the measured nitrogen solubility data in niobium and tantalum at 2243 K. The plasma consisted of excited and ionized nitrogen atoms and molecules and the excited metal and helium atoms. The electron density in the plasma was low, and the average kinetic energy of the electrons was determined to be about 0.6 ev. In the plasma environment, the solubilities of nitrogen in solid tantalum and niobium were about three times the corresponding equilibrium solubilities under nonplasma

conditions. The activity of nitrogen in the plasma, calculated from the nitrogen solubility data in the metals, is about an order of magnitude higher than the partial pressure of nitrogen in the plasma source gas. The solubility of a species in a condensed phase exposed to a plasma can be used to determine its activity in the plasma.

APPENDIX I

Collision processes in the formation of excited and ionized nitrogen in the plasma

It is believed[24] that the N_2^+ ions act as precursors in the formation of the nitrogen atoms. The formation of N_2^+ ions can take place through two different collision processes. The first one involves collision of nitrogen molecules with energetic electrons according to the following reaction:[24]

$$N_2 + e_f^- = N_2^+ + 2e^- \qquad [Ia]$$

where e_f^- denotes a fast electron with at least 15.6 eV energy which is much higher than the average kinetic energy of the electrons and, therefore, possessed by only a small population of electrons in the plasma. The second mechanism for the formation of N_2^+ ions involves Penning ionization, where metastable He atoms collide with N_2 molecules to cause ionization as follows:

$$N_2 + He^* = N_2^+ + He \qquad [Ib]$$

where He* denotes a metastable He atom with at least 19.8 eV energy. For the optical emission indicated in Table I at 587.57 nm, the upper energy level of He emission is 23.07 eV. Thus, the formation of N_2^+ ions can take place by both Reactions [Ia] and [Ib].

The N_2^+ ions collide with electrons to form excited nitrogen atoms of ^2D and ^2P states according to the following reactions:

$$N_2^+ + e_f^- = N(^2D) + N(^2D) \qquad [Ic]$$

$$N_2^+ + e_f^- = N(^2D) + N(^2P) \qquad [Id]$$

Reaction [Ic] releases 1.08 eV and is energetically favorable. However, Reaction [Id] requires an additional energy of 0.11 eV, which can be easily supplied by an electron. Although nitrogen atoms with (^2P) configuration were detected in the spectra, no N(^2D) peaks were observed. This is because the average life span[23] of N(^2D) atoms is 8 hours, which implies high stability of atoms in this energy state.

The extent of equilibrium thermal dissociation of nitrogen molecules to atoms at a sample temperature of 2243 K and 1.12 Pa is about 0.17 pct. Since the heavy particle temperature in the plasma is lower than the sample temperature, the extent of thermal dissociation in the plasma is small. The dissociation which is generally in excess of 10 pct in glow discharge plasmas[25] is the result of various collision processes.

The N^+ ions detected in the spectra can form in several ways. The collision processes involved are described by the following reactions:

$$N + e_f^- = N^+ + 2e^- \qquad [Ie]$$

$$N_2^+ + N_2 = N^+ + N + N_2 \qquad [If]$$

$$N_2 + e_f^- = N^+ + N + 2e^- \qquad [Ig]$$

The energies required for Reactions [Ie] through [Ig] are 14.53 eV, 17.4 eV, and 24.1 eV, respectively. Thus, the formation of N^+ ions is more favorable energetically from nitrogen atoms than from nitrogen molecules.

APPENDIX II

Calculation of ln (I/gAv) from experimental data

A sample calculation for determining ln (I/gAv) is shown below. The calculation is performed for the excited He peak at 587.57 nm. The base width of a peak, Δv, is calculated as

$$\Delta v = C(1/\lambda_1 - 1/\lambda_2) \qquad [IIa]$$

where C is the velocity of light and λ_1 and λ_2 are the wavelengths corresponding to the two ends at the base of the peak, which are 587.115 and 588.02 nm, respectively. Therefore, $\Delta v = 3 \times 10^{17}(1/587.115 - 1/588.02) = 7.86 \times 10^{11}\ s^{-1}$. The area under the peak, I, is taken as the product of half base width and the peak height, I_r = 68,095, and is multiplied by a y-axis calibration factor, CF = 0.75, predetermined for the particular fiber optic cable-optical multichannel analyzer combination at a wavelength of 587.57 nm.

$$\begin{aligned} I &= 0.5 \times \Delta v \times I_r \times \mathrm{CF} \\ &= 0.5 \times 7.86 \times 10^{11} \times 68{,}095 \times 0.75 \\ &= 2.00 \times 10^{16}\ s^{-2} \end{aligned} \qquad [IIb]$$

The value of ln (I/gAv) is then calculated from the computed value I and the values of g and A presented in Table II at a given frequency, v, as follows:

$$\begin{aligned} \ln(I/gAv) &= \ln[2 \times 10^{16}/(15 \times 0.706 \times 10^8 \\ &\qquad \times 5.1 \times 10^{14})] \\ &= -17.11 \end{aligned} \qquad [IIc]$$

APPENDIX III

Role of Doppler broadening

The contribution of the Doppler broadening is insignificant under the experimental conditions reported in this article. The full half width due to Doppler broadening[17] can be written as

$$\Delta\lambda_{1/2} = 7.16 \times 10^{-7}\lambda(T/M)^{1/2} \qquad [IIIa]$$

where $\Delta\lambda_{1/2}$ is the full half width due to Doppler broadening in Angstroms, λ is the wavelength in Angstroms, T is the electron temperature in Kelvin, and M is the atomic weight. Considering the neutral He peak at 447.15 nm, the full half width due to Doppler broadening amounts to only 0.107 Å at an electron temperature of 4455 K. At this wavelength, the full half width of the observed peak is 2.99 Å. Thus, the Doppler broadening is not important in the experimental conditions used for this investigation.

ACKNOWLEDGMENT

This work was supported by the United States Department of Energy, Office of Basic Energy Sciences, Division of Materials Science, under Grant Number DE-FGO2-84ER45158.

REFERENCES

1. R. Miller and T. DebRoy: *J. Appl. Phys.*, 1990, vol. 68 (5), pp. 2045-50.
2. M.M. Collur and T. DebRoy: *Metall. Trans. B*, 1989, vol. 20B, pp. 277-86.
3. P. Sahoo and T. DebRoy: *Metall. Trans. B*, 1987, vol. 18B, pp. 597-601.
4. P. Sahoo, M.M. Collur, and T. DebRoy: *Metall. Trans. B*, 1988, vol. 19B, pp. 967-72.
5. P. Sahoo and T. DebRoy: *Mater. Lett.*, 1988, vol. 6 (11), pp. 406-08.
6. M. Uda, S. Ohno, and T. Wada: *J. Jpn. Weld. Soc.*, 1969, vol. 38, pp. 382-92.
7. S. Ohno and M. Uda: *Trans. Nat. Res. Inst. Met.*, 1981, vol. 23, pp. 243-48.
8. J.D. Katz and T.B. King: *Metall. Trans. B*, 1989, vol. 20B, pp. 175-85.
9. T. Zacharia, S.A. David, J.M. Vitek, and T. DebRoy: *Weld. J. Res. Suppl.*, 1989, vol. 68 (12), pp. 499-509.
10. T. Zacharia, S.A. David, J.M. Vitek, and T. DebRoy: *Weld. J. Res. Suppl.*, 1989, vol. 68 (12), pp. 510-19.
11. H.G. Kraus: *Weld. J. Res. Suppl.*, 1989, vol. 68 (7), pp. 269-79.
12. M.M. Shahin: *J. Chem. Phys.*, 1965, vol. 43, pp. 1798-1805.
13. W.L. Wiese, M.W. Smith, and B.M. Glennon: *Atomic Transition Probabilities, Vol. I*, National Bureau of Standards, Gaithersburg, MD, 1966, pp. 48-76.
14. R.W.B. Pearse and A.G. Gaydon: *The Identification of Molecular Spectra*, John Wiley and Sons, Inc., New York, NY, 1941, pp. 137-42.
15. P.W.J.M. Boumans: *Theory of Spectrochemical Excitation*, Hilger and Watts, London, 1966, pp. 103-06.
16. J.A. Thornton: in *Deposition Techniques for Films and Coatings: Developments and Applications*, R.F. Bunshah, J.M. Blocher, Jr., T.D. Bonifield, J.D. Fish, P.B. Ghate, B.E. Jacobson, D.M. Mattox, G.E. McGuire, M. Schwartz, J.A. Thornton, and R.C. Tucker, Jr., eds., Noyes Publications, Park Ridge, NJ, 1982, pp. 19-62.
17. H.R. Griem: *Plasma Spectroscopy*, McGraw-Hill Book Company, New York, NY, 1964, pp. 303-12, 450-51, and 539.
18. W.L. Wiese: in *Plasma Diagnostic Techniques*, R.H. Huddlestone and S.L. Leonard, eds., Academic Press, New York, NY, 1965, pp. 268-69 and 272-75.
19. R. Reif: in *Handbook of Plasma Processing Technology*, S.M. Rossnagel, J.J. Cuomo, and W.D. Westwood, eds., Noyes Publications, Park Ridge, NJ, 1990, pp. 260-84.
20. Eckehard Fromm and Hermann Jehn: *Metall. Trans.*, 1972, vol. 3, pp. 1685-92.
21. V.P. Elyutin, D.G. Maksimov, and E.I. Mozzhukhin: *Russian Metallurgy*, 1972, no. 6, pp. 49-51.
22. V.S. Nguyen: in *Handbook of Thin-Film Deposition Processes and Techniques*, K. Schuegraaf, ed., Noyes Publications, Park Ridge, NJ, 1988, pp. 112-46.
23. H. Dun, P. Pan, F.R. White, and R.W. Douse: *J. Elect. Soc., Solid State Science and Technology*, 1981, vol. 128 (7), pp. 1555-63.
24. S.K. Mitra: *Phys. Rev.*, 1953, vol. 90, pp. 516-22.
25. T.D. Bonifield: in *Deposition Technologies for Films and Coatings: Developments and Applications*, R.F. Bunshah, J.M. Blocher, Jr., T.D. Bonifield, J.D. Fish, P.B. Ghate, B.E. Jacobson, D.M. Mattox, G.E. McGuire, M. Schwartz, J.A. Thornton, and R.C. Tucker, Jr., eds., Noyes Publications, Park Ridge, NJ, 1982, pp. 365-84.